Desalination and Water Treatment
www.deswater.com
doi: 10.5004/dwt.2017.1715

58 (2017) 285–297
January

Kinetic, equilibrium and thermodynamic studies for the adsorption of methyl orange using new anion exchange membrane (BII)

Muhammad Imran Khan[a], Muhammad Ali Khan[b], Shagufta Zafar[c], Muhammad Naeem Ashiq[d,*], Muhammad Athar[d], Ashfaq Mahmood Qureshi[d], Muhammad Arshad[e]

[a]*School of Chemistry and Material Science, University of Science and Technology of China, Hefei 230026, Anhui, China, Email: emran@mail.ustc.edu.cn*
[b]*Fujian Institute of Research on Structure of Matter, Chinese Academy of Sciences, Fuzhou 350002, China, Email: malichem92@fjirsm.ac.cn*
[c]*Department of Chemistry, the Government Sadiq College Woman University Bahawalpur, Bahawalpur 63000, Pakistan, Email: shagutazafar25.sz@gmail.com*
[d]*Institute of Chemical Sciences, Bahauddin Zakariya University, Multan-60800, Pakistan, Tel. +92-3009879344; Fax: +92-61-9210068; email: naeemashiqqau@yahoo.com, naeembzu@bzu.edu.pk (M.N. Ashiq), athar.qr@gmail.com (M. Athar), shamashfaq@yahoo.com (A.M. Qureshi),*
[e]*Institute of Chemistry, University of The Punjab, Lahore*

Received 8 December 2015; Accepted 3 June 2016

ABSTRACT

The adsorption of methyl orange (MO) from aqueous solution by anion exchange membrane BII was investigated at room temperature using batch technique. The anion exchange membrane was characterized by fourier transform infrared (FTIR) spectroscopy, scanning electron microscopy (SEM) and X-ray diffraction (XRD) techniques. The effect of various physico-chemical parameters such as contact time, membrane dosage, initial dye concentration, temperature and ionic strength on the removal of dye was investigated. Various kinetic models such as Lagergren's pseudo-first-order, pseudo-second-order, liquid film diffusion, Elovich, modified Freundlich and Bingham were applied to the adsorption data and it was observed that the adsorption of MO follow the pseudo second order kinetic model. Linear forms of adsorption isotherm models such as Langmuir, Freundlich, Tempkin and Dubinin–Radushkevich (D–R) were used to reveal experimental data and the results indicate that the adsorption of MO on anion exchange membrane BII fitted well to the Langmuir isotherm model. Thermodynamic parameters such as change in Gibbs free energy (ΔG), Change in enthalpy (ΔH) and Change in entropy (ΔS) were also determined. The negative values of ΔG and ΔH showed that the adsorption of MO on anion exchange membrane was spontaneous and exothermic process in nature.

Keywords: Adsorption; Methyl orange; Anion exchange membrane; Langmuir isotherm; Thermodynamics

* Corresponding author.

1. Introduction

Synthetic dyes are mostly employed for *textile dyeing*, leather dyeing, color photography, paper printing and as additives in petroleum product [1]. Reactive dyes are the most common dyes used because of their importance, such as bright colors, excellent color fastness and ease of application [2,]. They have different chemical structures. It depends on substituted aromatic and heterocyclic groups. A large number of reactive dyes are azo compounds that are linked by an azo groups [3]. Methyl Orange (MO) is a water-soluble azo dye which is widely used in the textile, printing, paper manufacturing, pharmaceutical, food industries and also as an acid base indicator due to its ability to function as weak acid [4]. Microbial succession and intestinal enzyme activities in the developing rat have also been studied for the MO and the dye is found to increase their nitro reductase and azo reductase activities significantly with the appearance of anaerobes in the large intestine. Azo dyes are well known carcinogenic organic substances. MO has various harmful effects on human beings as well on the aquatic life. It may cause eye or skin irritation, or inhalation may cause gastrointestinal irritation with nausea, vomiting, and diarrhea [5]. The presence of dyes in the water bodies may prevent the penetration of sunlight necessary for the photosynthesis process of aquatic plants. Thus, the safe removal of such a dye is the prime aim of our present research.

Several methods have have been used for the decoloration and degradation of dyestuff from wastewater, including electro-oxidation, advanced oxidation processes (AOPs), coagulation and flocculation, adsorption, biological degradation and membranes processes. Adsorption is one of the most useful and cheap method of color removal. Several types of materials were therefore investigated as the possible alternatives [6], ZnO and gold nanopaticles loaded activated carbon [7, 8], graphitic oxide [9]), and agriculture/industrial solid wastes (cocout husk [10, 11], maize cob [12] tin sulfide nanoaprticle load activated carbon [13] as easily available, cost effective, and eco-friendly adsorbents. Their price and efficiency vary from one adsorbent to other.

In recent years, commercial anion exchange resins have been shown to possess excellent adsorption capacity and demonstrate efficient regeneration property for the removal and recovery of reactive dyes [14, 15]. Due to the anion exchange resins tested were in the form of particle, their packed-bed operations would suffer from certain disadvantages (e.g slow pore diffusion, low accessible flow rate, high pressure drop and flow channeling). To remove the above limitations, anion exchange membranes, instead of resin particles, were successfully used to remove the anionic reactive dyes Cibacron blue 3GA and Cibacron red 3BA from water [16]. The macroporous membrane system can not only remove the technical problems of packed-bed operation but also exhibit the property of simple scale-up by simple stacking more membranes together or using a large membrane area. Thus ion exchange membrane becomes an excellent choice of adsorbent for industrial application.

In this paper , anionic dye MO is used as typical pollutant and anion exchange membrane BII was employed as an excellent adsorbent for removal of MO dye from aqueous solution. The effect of parameters such as contact time, amount of adsorbent, initial dye concentration, temperature and ionic strength on removal of dye from aqueous solution were also investigated. The adsorption kinetics, isotherms and thermodynamics for anionic dye MO on anion exchange membrane was also studied to look into the mechanism, adsorption capacity and feasibility of the process.

2. Experimental

2.1. Adsorbent

The commercial anion exchange membrane BII provided by Chemjoy Membrane Co. Ltd, Hefei, Anhui, China was used as adsorbent. It was prepared from blends of PVA and QPPO. It was used without further treatment. The pieces of membranes used for the adsorption studies have the length of 3 cm, width 2.5 cm and thickness of 0.182 mm. The area resistance of the membrane was found to be 1.7 ohm cm^2. The ion exchange capacity (IEC) and water uptake (W_R) of anion exchange membrane BII are 0.38 mmol/g and 41.6%, repectively.

2.2. Adsorbate

The commercial anionic dye known as methyl orange (MO) (C.I. 13025, MF: $C_{14}H_{14}N_3NaO_3S$, 327.34 g mol^{-1}, λ maximum 464 nm) was obtained from Fluka chemicals and used as adsorbent. Its solubility is 0.5 g/100 mL. The stock solution of 1000 mg/L was prepared by dissolving 1.0 g of accurately weighed MO in 1 liter of double distilled water and required concentrations were obtained by further dilution of stock solution. All the chemicals used in the experiments were of analytical reagent grade. The dye structure was shown in Fig. 1.

2.3. Adsorption

Adsorption isotherms provide important informations on the adsoprtion capacity of the adsorbents and the type of adsorbent-adsorbate intraction. Batch adsorption of methyl orange (MO) dye was carried out by immersing anion exchange membrane (BII) into measured volume of dye aqueous solution at room temperature. The bottles were shaked at constant speed of 120 rpm. The concentration of MO was determined by UV/VIS spectrophotometer (UV-2550, SHIMADZU) and related calibration curves were obtained. The wavelength used for MO

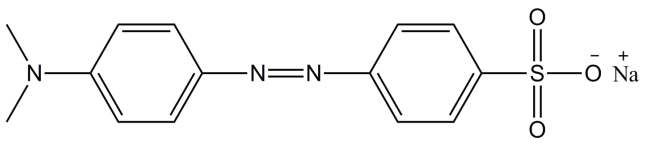

Fig. 1.Chemical strucure of Methyl orange (MO) dye.

was 464 nm. The MO adsorption on BII at time *t*, was calculated by Eq. (1):

$$q_t = \frac{C_o - C_t}{W} \times V \quad (1)$$

where C_o and C_t are the concentration of MO at initial state and at time t respectively. Similarly *V* and *W* are volume of MO aqueous solution and weight of adsorbent, respectively. Thermodynamic parameters represent the feasibility and spontaneity of adsorption process. The thermodynamics parameters such as Gibbs free energy, entropy and enthalpy of adsorption was also calculated and discussed.

2.4. Membrane characterization

2.4.1. FTIR spectra

FTIR spectra of dried membranes were recorded by using the technique attenuated total reflectance (ATR) with FTIR spectrometer (Vector 22, Bruker) having resolution of 2 cm^{-1} and a total spectral range of 4000–400 cm^{-1}.

2.4.2. Microscopic characterizations

Membrane morphological characterization was successfully done through a field emission scanning electron microscope (FE-SEM, Sirion200, FEI Company, USA). Surface and cross-sectional views of membranes were taken from dry membranes. The SEM images used anion exchange membranes was shown as representative cases.

2.4.3. XRD analysis

The X-ray diffraction data for finely ground samples were collected at 298 K on a Rigaku MiniFlex II diffractometer with Cu Kα radiation in the 2θ range of 3–60°.

3. Result and discussions

3.1. Membrane characterization

The surface properties of adsorbent (anion exchange membrane BII) were investigated FTIR, scanning electron microscopy and X-ray diffraction technique. Their details are given below:

3.1.1. FTIR analysis

Fig. 2 shows the FTIR spectrum of anion exchange membrane used in the adsorption of MO from aqueous solution at room temperature. These spectra have number of peaks representing the structure of used membrane in the present work. The peak observed at 2900 cm^{-1} corresponds to $-CH_3$ stretching from the PPO back bone [17]. The broad peak in the range of 3050-3600 cm^{-1} is because of OH group in the membrane [17]. The band in the region of 1620 cm^{-1} corresponds to the stretching vibration of C-N group [18]. The adsorption peaks of symmetrical and asymmetrical stretching vibration

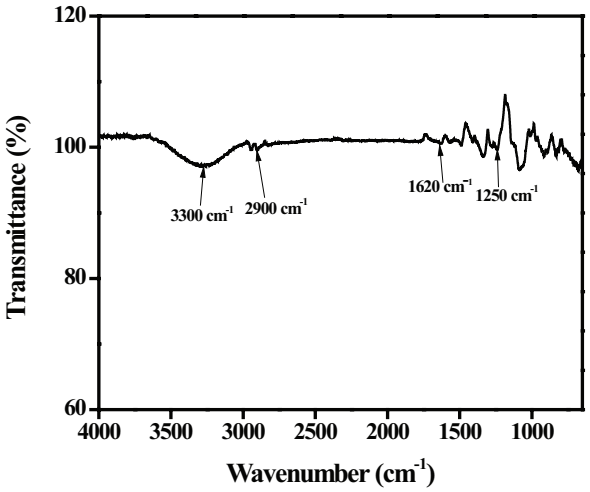

Fig. 2. FTIR spectrum of the prepared anion exchange membrane BII.

of C-O are at 1200 cm^{-1} and 1306 cm^{-1} and those of phenyl group at 1470 cm^{-1} and 1600 cm^{-1} respectively [17].

3.1.2. Membrane morphology

The morphology of anion exchange membrane BII was investigated by electron microscopy and the obtained micrograph is shown in Fig. 3. It can be seen from the membrane surface images that used membrane possess better miscibility. There are no holes, pores or cracks in the surface and cross-section of studied membranes. Overall, the anion exchange membrane BII possesses uniform surface with no visible pore in the surface and cross-section.

3.1.3. XRD analysis

The XRD data were analyzed using a profile fitting by a least-squares method employing the computer program GSAS implemented with EXPGU. The results are shown in Fig. 4. It shows that this is actually a new phase. XRD Comparison of the intercalated gallery height with that of the trimethyl amine measures the thickness of the PVA/trimethyl amine film. XRD scans for the corresponding d-spacing distributions for the concentrations. The distribution of the intercalated d-spacing periodic assemblies of intercalated trimethyl amine layers; these are characterized by d-spacing, mixtures of PVA and trimethyl amine, suggesting the existence of exfoliated inorganic layers throughout the polymer BPPO matrix. Wide angle XRD provides evidence that we actually have a new phase membrane in the composite. Thus, XRD consistently show that these samples are in a hybrid structure where both intercalated and exfoliated layers coexist in considerable ratios.

3.2. Effect of operating parameters

The effect of operating parameters such as contact time, mmbrane dosage, initial dye concentration, temperature and

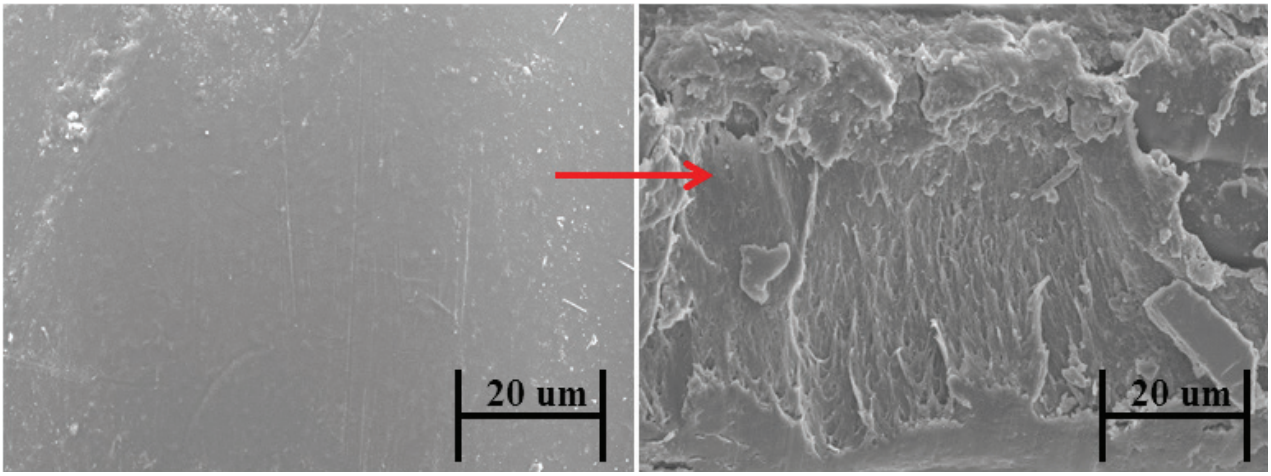

Fig. 3. SEM images of the anion exchange membrane BII.

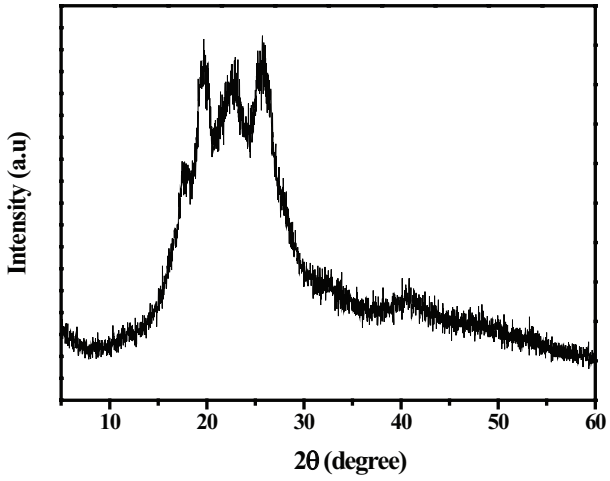

Fig. 4. XRD pattern for the prepared membrane.

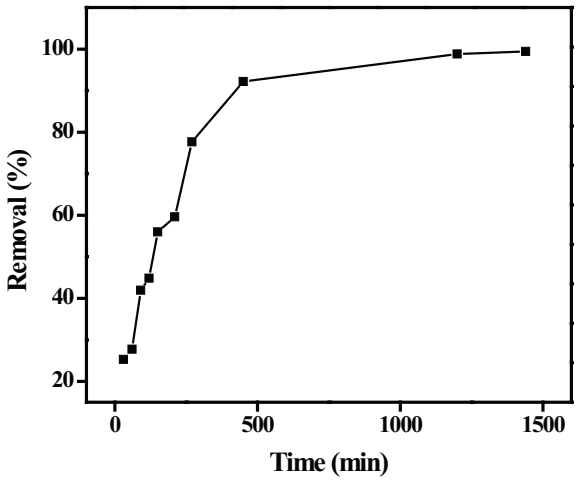

Fig. 5. Effect of contact time on the removal of MO from aqueous solution by anion exchange membrane BII.

ionic on the removal of MO dye from aqueous solution has been investigated. Their details are given below.

3.2.1. Effect of contact time

The effect of contact time on the percentage removal of MO was studied keeping the shaking speed (120 rmp), concentration of adsorbate (50 mg/L), amount of adsorbent constant at room temperature. It is clear that the removal of MO dye increases with contact time as shown in Fig. 5 and get saturation in 24 hours. It indicated that the adsorption process was initially very fast and which gradually slows down and attaind equilibrium whitin 24 hours. As this is the maximum time where all the dye molecules which were present get adsorbed on the membrane so this optimum contact time was used for further experiments. The fast dye removal in the initial stage was due to higher number of available vacant sites on the surface of adsorbent which gets saturated as time passes out. Similar results have been previously reported in the literature for dye removal [19].

3.2.2. Effect of membrane dosage

The influence of adsorbent dosage is significant to study the maximum adsorption with small possible amount of adsorbent. The effect of the membraene dosage on the percentage removal of MO dye was investigated keeping the other factors such as contact time, initial dye concentration, shaking speed and temperature constant. It has been observed that the removal of MO dye increases with increasing membrane dosage. The results are shown in Fig. 6. The removal of MO dye increased from 63.28% to 99.40% with increasing membrane dosage from 0.02 g to 0.1 g. The maximum removal of the methyl orange was obtained at 0.04 g of membrane dosage ad no significant increase in percentage removal was observed so this amount of the membrane was used for further investigations of parameters. The increase in percent adsorption was due to number of available active sites inceases with increasing the membrane dosage. Similar results have been previously reported in the literature [20]. However, further increment in the adsorbent dosage did not

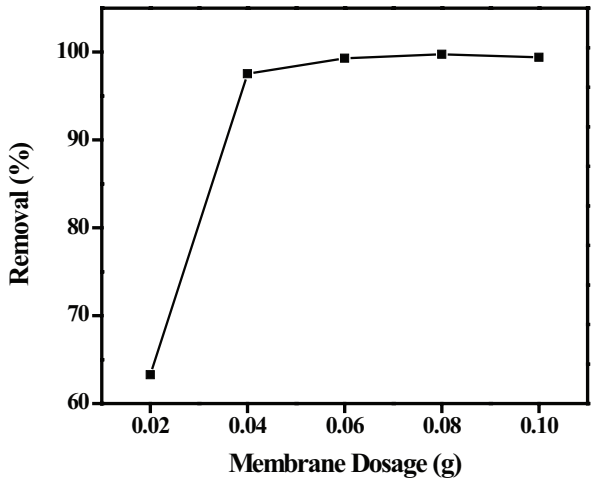

Fig. 6. Effect of membrane dosage on the removal of MO from aqueous solution by anio exchange membrane BII.

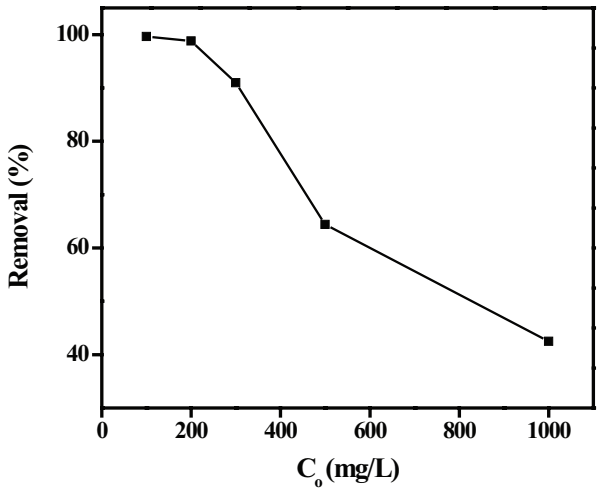

Fig. 7. Effect of initial dye concentration on the removal of MO from aqueous solution by anion exchange membrane BII.

give any significant changes in the percentage removal and this could be due to the saturation of binding sites [21].

3.2.3. Effect of initial dye concentration

The influence of intial dye concentration on the removal of MO was investigated keeping the other factors such contact time, membrane dosage, shaking speed and temperature constant. The effect of initial dye concentration on the removal of MO was investigated and results are shown in Fig. 7. It is clear that the removal of MO decreases from 99 to 40% with initial dye concentration when dye concentration was increased from 200 to 1000 mg/L. This is due with increase in MO concentration the ratio between the available sites and dye molecules for adsorption was increased resulting saturation of active sites of adsorbent and hence percentage removal was decrease.

3.2.4. Effect of temperature

The influnce of temperature on the percentage removal of MO from aqueous solution was investigated keeping the contact time, membranes dosage, stirring speed, solution volume and concentration (50 mg/L) constant and results are represented in Fig. 8. It has been observed that the removal of MO decreases with increasing temperature. The percentage removal of MO decreases from 99.45% to 96.31% with increasing the temperature from 393K to 323 K. These results represent that removal of MO by anion exchange membrane was exothermic process and more favourable at low temperature.

3.2.5. Effect of ionic strength

It is an important factor that controls both the electrostatic and nonelectrostatic intractions between the dye and the membranes surface. The effect of ionic strengh on the removal of MO from aqueous solution was studied by addition of different amount of sodium chloride to the dye solution and results are shown in Fig. 9. It can be observed from Fig. 9 that the removal of MO dye decreases with increasing the

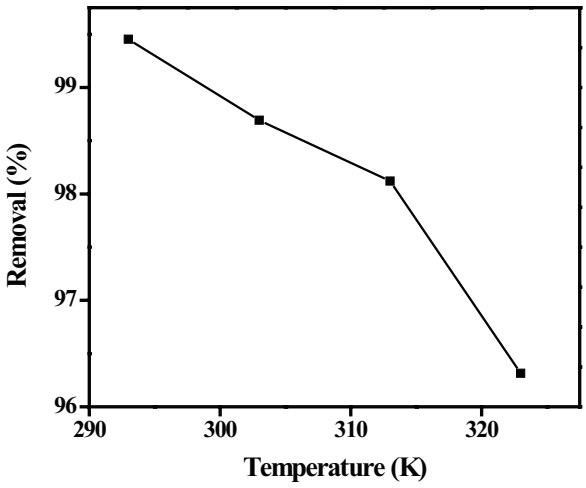

Fig. 8. Effect of temperature on the removal of MO from aqueous solution by anion exchange membrane BII.

concentration of salt. The removal of dye dereases from 95.57% to 71.43% with increasing the concentration of salt from 0.2 M to 1.5 M . This could be due to the competition between the MO anions and Cl^- for the active sorption sites [22].

3.3. Adsorption kinetics

Several adsorption models are used to study the controlling mechanism of adsorption process such as chemical reaction and diffusion control.

3.3.1. Pseudo-first-order model

The linearized form of the Lagergren Pseudo-first-order rate equation is given by [23]:

$$loq(q_e - q_t) = \log q_e - \frac{K_1 t}{2.303} \quad (2)$$

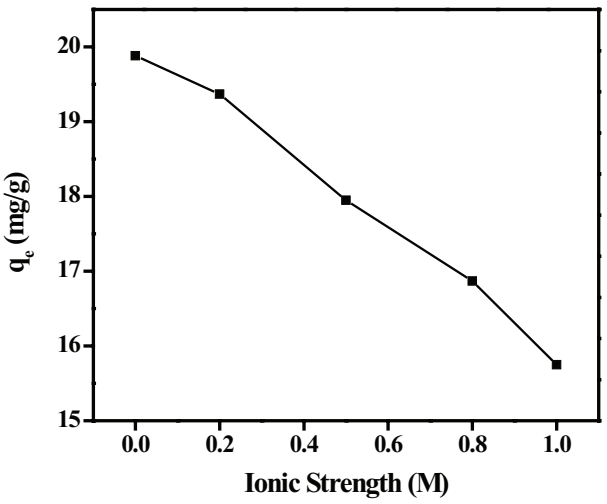

Fig. 9. Effect of ionic strength on the removal of MO from aqueous solution by anion exchange membrane BII.

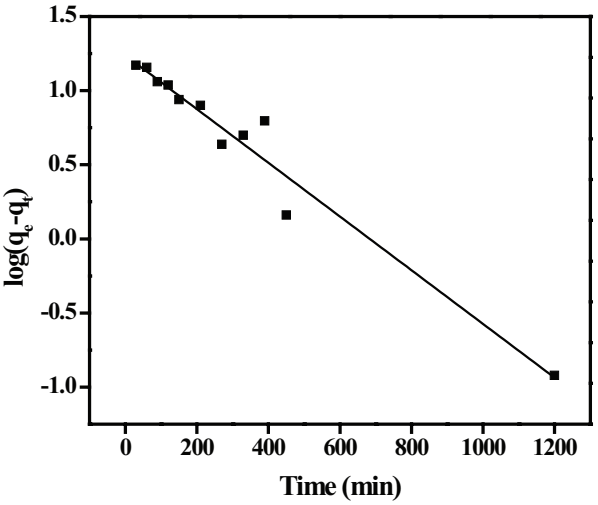

Fig. 10. Pseudo-first-order kinetics for adsorption of MO on anion exchange membrane BII.

where q_e and q_t is the amount of adsorbate adsorbed at equilibrium and time t repectively and k_1 (/min) is the rate constant of pseudo-first-order adsorption model. The plot of $\log(q_e - q_t)$ vs time for MO asorption on BII is given in Fig. 10. The value k_1 is obtained from slope of Fig. 10 and given in Table 1. These plots are linear, however the linearity of these curves does not necessarily assure the mechanism due to the inherent disadvantage of correctly estimating equilibrium adsorption capacity [24]. The correlation cofficient (R^2) value for MO adsorption on BII is 0.952. Moreover, there is a large difference between experimental adsorption capacity ($q_{e,\exp}$) and calculated adsorption capacity values ($q_{e,\text{cal}}$), therefore pseudo-first-order model does not explain the rate process.

3.3.2. Pseudo-second-order model

The linearized form of pseudo-second kinetic model is expressed as [25]:

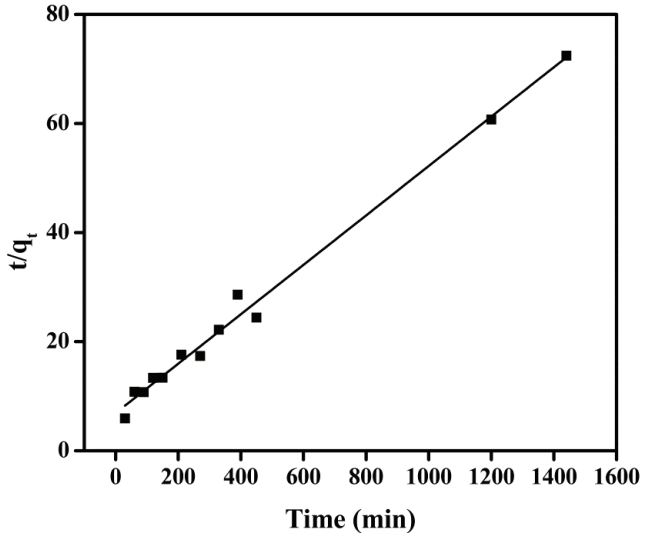

Fig. 11. Pseudo-second-order kinetics for adsorption of MO on anion exchange membrane BII.

$$\frac{t}{q_t} = \frac{1}{k_2 q_e^2} + \frac{t}{q_e} \tag{3}$$

where k_2 (g/mg.min) is the rate constant of pseudo-second-order model. The graphical representation of pseudo-second-order model is shown in Fig. 11. The value of adsorption capacity (q_e) can be calculated from slope of Fig. 11 and are given in Table 1. This value of adsorption capacity is in good agreement with the experimental value (19.88 mg/g). The value of correlation cofficient is ($R^2 > 0.99$) which shows that experimental data fitted well to the pseudo-second-order model.

3.3.3. Elovich model

The most interesting model to describe the activated chemisorption is the Elovich equation [26]:

$$q_t = \frac{1}{\beta}\ln(\alpha\beta) + \frac{1}{\beta}\ln t \tag{4}$$

where α (mg/g.min) and β (g/mg) are constant. The parameter α is considered as initial sorption rate (mg/g.min) and β is related to the extent of surface coverage and activation energy for the chemisorption. The plot of q_t vs lnt for Elovich model is given in Fig. 12. The values of α and β are calculated from intercept and slope of Fig. 12 and are given in Table 1. The values of correlation cofficient (R^2) were 0.927 lower than that of pseudo-second-order model.

3.3.4. Liquid film diffusion model

The liquid film model is expressed as [27]:

$$Ln(1-F) = -K_{fd}t \tag{5}$$

where K_{fd} is liquid film diffusion rate constant, and $F = q_t/q$. The plot of ln(1–F) vs time for liquid film model is shown in Fig. 13. The value of K_{fd} is measured from slope of Fig. 13

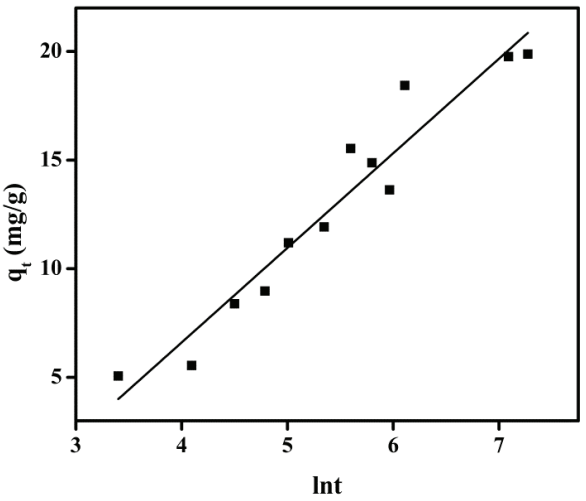

Fig. 12. Elovich model for adsorption of MO on anion exchange membrane BII.

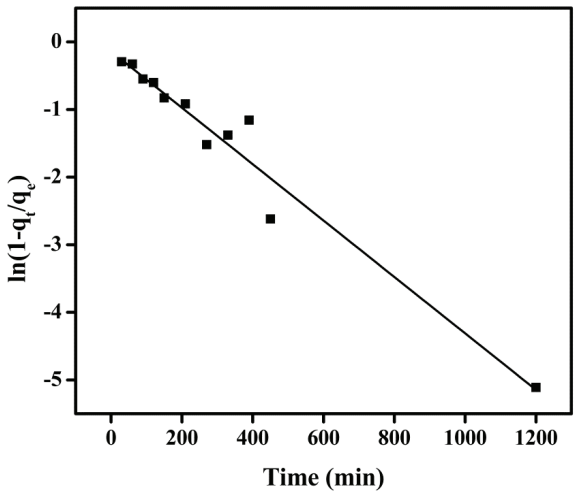

Fig. 13. Liquid film diffusion model for adsorption of MO on anion exchange membrane BII.

and are shown in Table 2. The value of correlation coefficient (R^2) is 0.952 for MO adsorption on BII which is lower than pseudo-second-order model. It shows that liquid film diffusion model is not suitable to explain the experimental data.

3.3.5. Modified Freundlich equation

The modified freundlich equation was orignally developed by Kuo and Lotse [28]:

$$q_t = kC_o t^{1/m} \tag{6}$$

where q_t is amount of adsorbed dye (mg/g) at time t, k apparent adsorption rate constant (L/g.min), C_o the initial dye concentration (mg/L), t the contact time (min) and m is the Kuo-Lotse constant. The values of k and m were used to eualuate the effect of dye surface loading and ionic strength on the adsorption process.

Linear form of modified Freundlich equation given as:

$$\ln q_t = \ln\left(kC_o\right) + \frac{1}{m}\ln t \tag{7}$$

The graphical representation of modified Freundlich equation is given in Fig. 14. The parameters m and k are obtained from slope and intercept of Fig. 14 and are given in Table 2. The value of correlation coefficient for MO adsorption on anion exchange membrane BII is 0.899.

3.3.6. Bingham Equation

Bingham equation [29] is given as:

$$\log\log\left(\frac{C_o}{C_o - q_t m}\right) = \log\left(\frac{k_o m}{2.303V}\right) + \alpha \log t \tag{8}$$

where C_o is the initial concentration of dye solution (mg/L), V is volume of solution (mL), q_t is amount of dye adsorbed

Table 1
Pseudo-first-order, pseudo-second-order and Elovich model rate constants (q_e: mg/g; k_1: (/min); k_2: g/mg.min; α: mg/g.min; β: g/mg)

Pseudo-first-order				Pseudo-second-order			Elovich model		
$q_{e\,(exp)}$	$q_{e\,(cal)}$	$k_1 \times 10^{-3}$	R^2	q_e	$k_2 \times 10^{-4}$	R^2	α	β	R^2
19.88	17.38	1.81	0.952	22.07	2.97	0.991	0.36	0.23	0.927

Table 2
Liquid film diffusion model, modified Freundlich equation and Bingham equation rate constant (kfd: (/min); k : L/g.min; ko: mL/g/L)

Liquid film diffusion model			Modified Freundlich equation			Bingham equation		
$k_{fd} \times 10^{-3}$	C_{fd}	R^2	m	k	R^2	k_o	α	R_2
4.17	–0.14	0.952	2.56	0.049	0.899	1.13	0.39	0.899

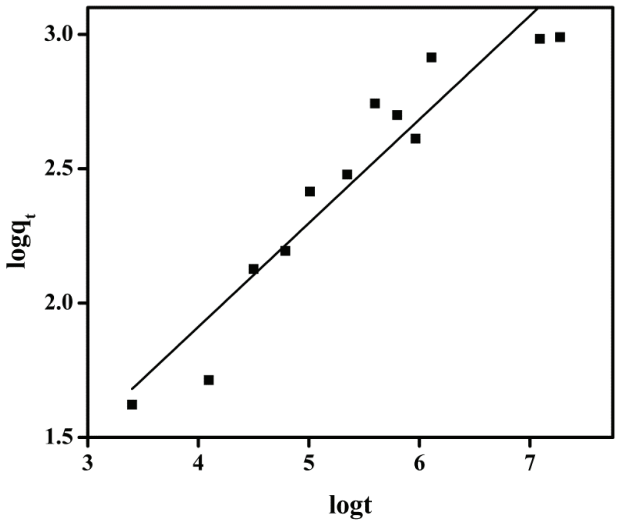

Fig. 14. Modified Freundlich equation plot between logt vs logq_t for adsorption of MO on anion exchange membrane BII.

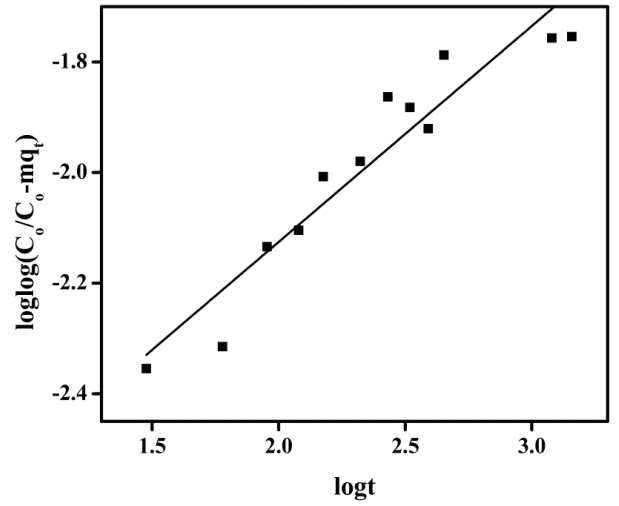

Fig. 15. Bangham equation plot between logt vs log log(Co/Co–mq_t) for adsorption of MO onanion exchange membrane BII.

(mg/g) at time *t*, m is weight of adsorbent used (g/L). α (<1) and k_o (mL/(g/L) are constants. The plot of loglog(C_o/C_o–q_t m) Vs logt for MO adsorption on anion exchange membrane BII is given in Fig. 15. The values of α and m are obtained from slope and intercept of Fig. 15 and are given in Table 2. The double logarithmic plot did not give linear curves for MO adsorption on anion exchange membrane BII indicating that the diffusion of adsorbate into pores of the sorbent is not the only rate controling step [30, 31]. It may be that both film and pore diffusion were important to different extent in the MO adsorption from aqueous solution.

3.3.7. Intraparticle diffusion model

Fick's 2nd law (Eq. (9)) has been used to see the possibility of intraparticle diffusion as rate limiting step and is given as [29]:

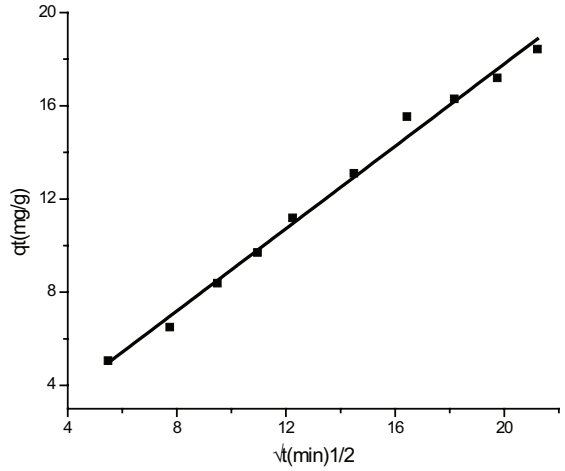

Fig. 16. Intraparticle diffusion plot for the adsorption of MO onto the anion exchange membrane.

$$q_t = k_{id}\sqrt{t} + I \tag{9}$$

where *I* is the boundary layer effect and k_{id} is the intraparticle rate constant. The value of k_{id} and I has been determined from the slope and intercept of the plot q_t versus $\sqrt{t}$, respectively as shown in fig. 16. It has been reported that the line of the plot q_t versus $\sqrt{t}$ should pass through origin (I = 0.0) if the intraparticle diffusion is the rate controlling step. In the present work, the value of *I* is found to be 0.13 which is greater than zero indicating that the surface adsorption and diffusion are concurrently operating.

3.4 Adsorption Isotherms

The adsorption isotherms are drawn between the quantity of dye adsorbed per gram of membranes "q_e" and the quantity of dye left in equilibrium solution C_e and is shown in Fig. 17**.** The adsorption isotherm shows that adsorption capacity "q_e" increases with the concentration of dyes. The adsorption isotherm shows the distribution of molecules between solid and liquid phases at equilibrium state. The analysis of isotherm data by fitting the data to different isotherm models is an important step in finding the most suitable model that can be used to describe the adsorption process [32]. There are several isotherm model to describe the isotherm data. Here, Langmuir, Freundlich Temkin and Dubinin–Radushkevich (D–R) isotherm models are used to reveal the experimental data. The Langmuir model depends upon the maximum adsorption coincides to the saturated monolayer of liquid (adsorbate) molecules on the solid (adsorbent) surface. The linear form of Langmuir model is given as follows [33]:

$$\frac{C_e}{q_e} = \frac{1}{bq_m} + \frac{C_e}{q_m} \tag{10}$$

where *b* is Langmuir constant (L/mg) and q_m is Langmuir monolayes adsorption capacity (mg/g), C_e is supernatant concentration at equilibrium state of the system (mg/L),

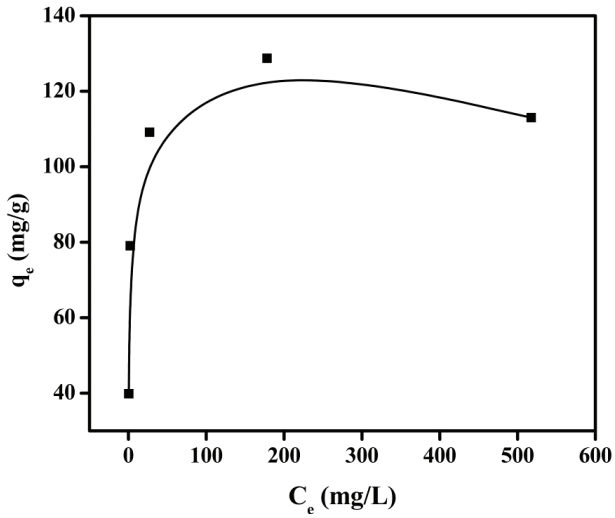

Fig. 17. Adsorption isotherm for adsorption of MO on anion exchange membrane BII.

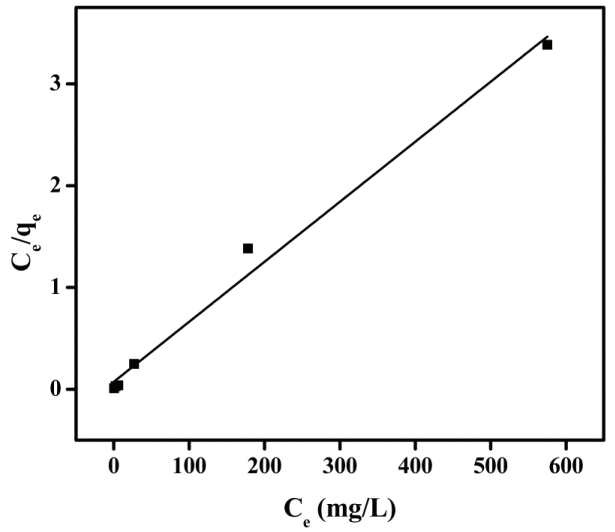

Fig. 18. Langmuir isotherm for adsorption of MO on anion exchange membrane BII.

and q_e is the amount of dye adsorbed at equilibrium state of system (mg/g). The plot of C_e vs C_e/q_e for Langmuir model is shown in Fig. 18. The values of q_m and b are calculated from slope and intercept of Fig. 18 and are given in Table 3. The correlation coefficient (R^2) value is 0.988 indicating that the adsorption of MO on BII fitted well to the Langmuir model.

The essential characteristics of Langmuir isotherm can be expressed in term of dimensionless constant separation factor R_L that is give by [34]:

$$R_L = \frac{1}{1+bC_o} \tag{11}$$

The value of R_L indicates the shape of the isotherm to be either unfavourable (R_L > 1), linear (R_L = 1), favourable

Table 3
Langmuir and Freundlich isotherm parameters (q_e: mg/g; b: L/mg)

Langmuir isotherm			Freundlich isotherm		
q_m	b	R^2	n_F	K_F	R^2
172.41	0.079	0.988	6.49	56.23	0.810

Table 4
Comparison of maximum adsorption qm (mg/g) of methyl orange on different adsorbents

S. No.	Adsorbent	q_m (mg/g)	Reference
01	Banana Peel	3.62	37
02	Bottom Ash	21.00	38
03	Multiwalled carbon nanotubes	52.86	39
04	Activated Clay	16.78	40
05	Modified Wheat Straw	50.40	41
06	Chitosan Nanocomposites	29.41	42
07	Orange peel	20.50	37
08	Lapindo Volcanic Mud	333.3	43
09	Aminated Pumpkin Seed Powder	143.70	44
10	Nitrogen doped mesoporous carbon material (NMC-2)	155.5	45
11	Chitosan Biomass	29.00	46
12	CuO/NaA Zeolite	79.49	47
13	Anionic membrane BII	172.41	Present work

(0 < R_L > 0), or irreversible (R_L= 0) [35]. The values of R_L for adsorption of MO on BII lies in the range (0.013–0.11) which are in between 0 and 1, therefore verifying the favourable adsorption process. Moreover, the low R_L values implied that the interaction of dyes molecules with BII might be relatively strong [36]. The value of maximum adsorption (q_m) in the present work is comapred with that of already reported for the adsorption of mothly orange onto different adsorbents and their values are tabulated in Table 4. It can be seen from table that the value of qm (172.41 mg/g) in the present work is much higher as comapred to most of the adsorbents already used which indicate that the anionic exchange membrane is an excellent adsorbent for the removal of methyl orange from the aqueous media.

The widely used Freundlich model is an empirical relation used to explain the heterogeneous system. The Freundlich isotherm model is expressed as [48]

$$\log q_e = \log K_f + \frac{1}{n}\log C_e \tag{12}$$

where K_f and n are Freundlich constant. The values of n and K_f are calculated from slope and intercept of Fig. 19 and given Table 3. The correlation coefficient (R^2) value is 0.810 showing that the adsorption data followed the Freundlich model. The value of Freundlich contant n decides the favourability of adsorption process. If the value of of n is in range from

1 to 10, the adsorption is favourable. The value of n for MO adsorption on BII was 6.49 indicating the favourable adsorption process.

The Tempkin isotherm assumes that heat of adsorption of all the molecules decrease linearly with the coverage of the molecules due to the adsorbate-adsorbate repulsion and the adsorption of adsorbate is uniformly distributed and that the fall in the heat of adsorption is linear rather than logarithmic [49]. It is expressed as:

$$q_e = B_T \ln A_T + B_T \ln C_e \quad (13)$$

where $B_T = R_T/b_T$, T is absolute temperature (K) and R is gas constant (8.31 J/mol.K). The constant b_T is related to the heat of adsorption and A_T is equilibrium binding constant coinciding to the maximum binding energy. The plot of q_e verses ln C_e for Tempkin model is given Fig. 20. The value of B_T and A_T are determined from slope and intercept of Fig. 20 and given in Table 5. The correltaion coefficient ($R^2 = 0.807$) of Tempkin isotherm is lower than the Langmuir Freundlich isotherm model representing that the adsorption of MO on anion exchange membrane BII is not fitted to the Tempkin model.

The adsorption data was applied to the Dubinin–Redushkevich (D–R) model to distinguish between physical and chemical adsorption [49]. The D–R model is expressed as:

$$Ln q_e = Ln q_m - \beta\varepsilon^2 \quad (14)$$

where β is the activity coefficient related to mean sorption energy and ε is the polanyi potential that is given as:

$$\varepsilon = RTLn\left(1+\frac{1}{C_e}\right) \quad (15)$$

where R is the universal gas constant (KJ/mol) and T is the absolute temperature (K). β is related to the mean adsorption energy by the following expression:

$$E = \frac{1}{\sqrt{2\beta}} \quad (16)$$

The plot of $Ln q_e$ vs ε^2 for D–R isotherm is given in Fig. 21. The mean adsorption energy (E) in the D–R isotherm can act as a rule to differentiate chemical and physical adsorption [50]. For magnitude of E between 8 KJ/mol and 16 KJ/mol, the adsorption process followed chemical ion exchange, and values of E below 8 KJ/mol were the characteristic of physical adsorption process [51].`The E value for MO adsorption on anion exchange membranes BII is 1.96 KJ/mol indicating that MO adsorption on BII followed physical adsorption.

3.5. Adsorption thermodynamics

The parameters namely as change in Gibb's free energy (ΔG), enthalpy (ΔH) and entropy (ΔS) were calculated from given relations:

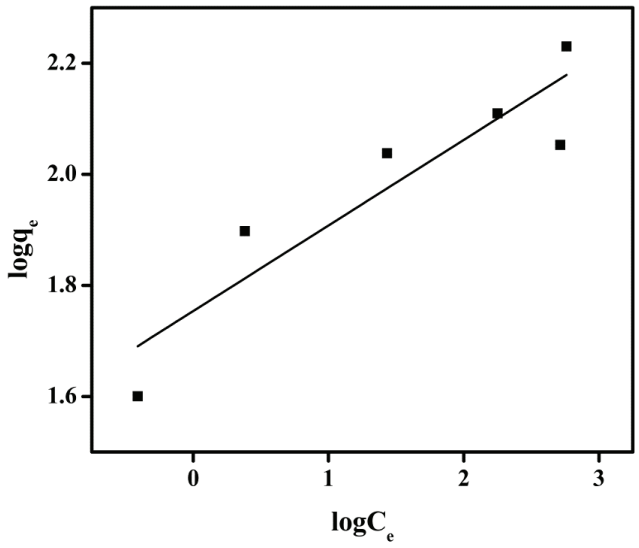

Fig. 19. Freundlich isotherm for adsorption of MO on anion exchange membrane BII.

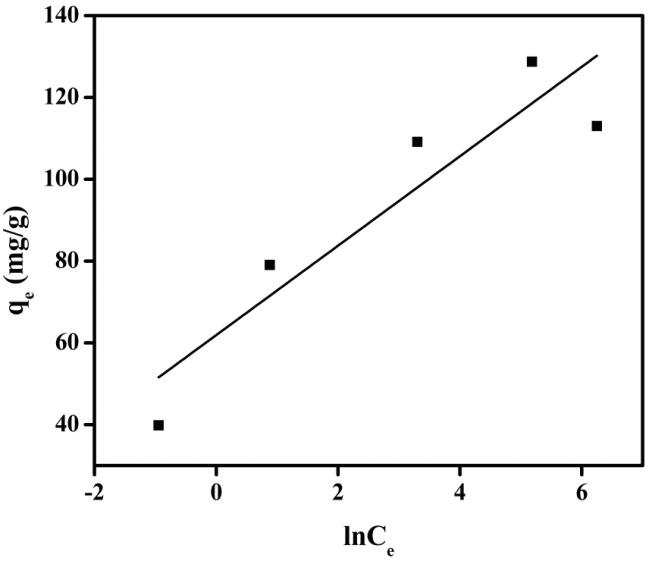

Fig. 20. Temkin isotherm for adsorption of MO on anion exchange membrane BII.

Table 5
Dubinin–Radushkevich Isotherm (D–R) and Tempkin isotherm parameters (B_T: J/mol; A_T: kg/mol; β: mol²/KJ²; E: KJ/mol)

Dubinin–Radushkevich isotherm				Temkin isotherm		
q_m	β	E	R^2	B_T	A_T	R^2
143.85	0.13	1.96	0.870	10.93	287.15	0.807

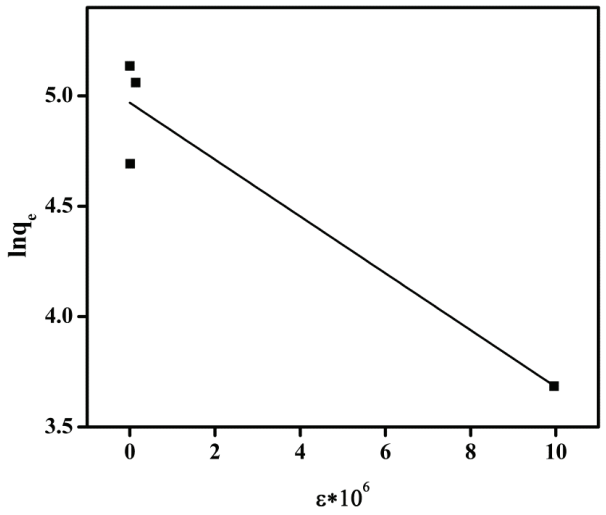

Fig. 21. Dubinin–Radushkevich (D–R) isotherm for adsorption of MO on anion exchange membrane BII.

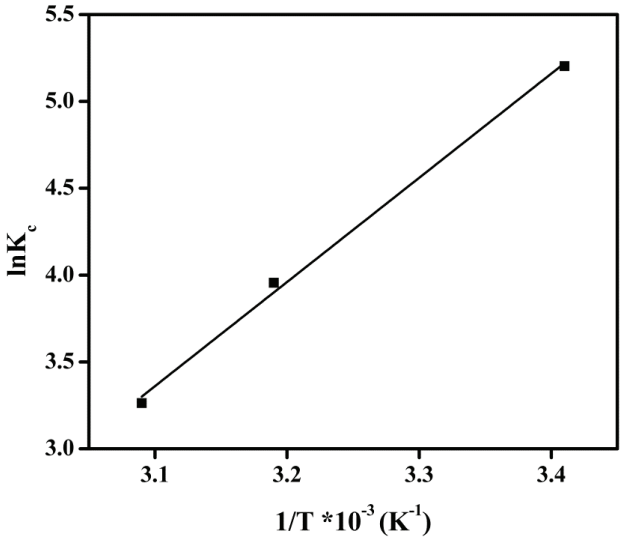

Fig. 22. Plot of 1/T vs lnKc for adsorption of MO on anion exchange membrane BII.

$$\ln Kc = \frac{\Delta S}{R} - \frac{\Delta H}{RT} \quad (17)$$

$$K_c = \frac{C_a}{C_e} \quad (18)$$

$$\Delta G = \Delta H - T\Delta S \quad (19)$$

where K_c, C_a, C_e, R, T are the the equilibrium constant, amount of dye (mol/L) adsorbed on the adsorbent per litre (L) of the solution at equilibrium, equilibrium concentration (mol/L) of dye in solution, general gas contant (8.31 J/mol.K) and absolute temperature (K) respectively. Similarly ΔG, ΔH and ΔS are the change in Gibb's free energy (KJ/mol), enthalpy (KJ/mol) and entropy (J/mol.K), respectively. The plots of $\ln K_c$ verses 1/T for adsorption of MO on anion exchange membrane BII is shown in Fig. 22. The adsorption enthalpy (ΔH^o) and entropy (ΔS^o) are calculated from slope and intercept of Fig. 22 and are given in Table 6. The values of Gibb's free energy (ΔG) are positive at all temperature studied and increases with temperature as represented Table 6. It might be because of intraction between adsorbent and adsorbate, with unbalanced competition imputed to heterogeneity of membrane surface and system got energy from external source at higher temperatures. The nagative value of enthalpy (ΔH) shows that the adsorption of MO on anion exchange membrane is exothermic process. Similarly the negative value of entropy (ΔS) indicates decrease in randomnes at the dye-membrane interface during the adsorption of MO on anion exchange membrane.

Table 6
Thermodynamic parameters for adsorption of MO on anion exchange membrane BII

ΔH (KJ/mol)	ΔS (J/mol)	–ΔG (KJ/mol)			
		293 K	303 K	313 K	323 K
–49.86	–126.56	37.03	38.29	39.56	40.82

4. Conclusions

The adsorption of methyl orange onto anion exchange membrane has been studied and it was found that the equilibrium was observed after 24 hours. The percentage removal of MO increase with the increase in membrane dosage and maximum removal of 99.4% was obtained at 0.4g of membrane. The removal of dye was decreased from 99 to 40% with the increase in initial concentration from 200 to 1000mg/L and from 99.45% to 96.31% with increasing the temperature from 393 K to 323 K. The adsorption capacity (q_m) in the present work was found to be 172 mg/g which is much higher as compared to those of reported in the literature. The value of E (1.96 KJ/mol) indicate that MO adsorption on BII followed physical adsorption. The negative values of ΔG and ΔH indicate that the adsorption process is spontaneous and exothermic. The value of adsorption capacity (172 mg/g) and percentage removal (99.4%) suggest that the anion exchange membrane BII is an excellent adsorbent for the removal of methyl orange from aqueous media.

Nomenclature

Code	—	Name
MO	—	Methyl orange
IEC	—	Ion exchange capacity, mmol/g
W_R	—	Water uptake, %
C_o	—	Initial Concentration of dye, mg/L
C_t	—	Concentration of dye at time t, mg/L
W	—	Weight of adsorbent, g
V	—	Volume of adsorbate, dm^3
k_1	—	Rate constant of pseudo-first-order model, /min
k_2	—	Rate constant of pseudo-second-order model, g/mg.min

α — Initial sorption rate, mg/g.min
β — Extent of surface coverage and activation energy for the chemisorption, g/mg
K_{fd} — Liquid film diffusion rate constant
k — Apparent adsorption rate constant, L/g.min
m — Kuo-Lotse constant
b — Langmuir constant, L/mg
q_m — Langmuir monolayes adsorption capacity, mg/g
K_f — Freundlich constant
T — Absolute temperature, K
R — Gas constant, 8.31 J/mol.K
b_T — heat of adsorption, J/mol
A_T — Equilibrium binding constant coinciding to the maximum binding energy, L/mg

References

[1] K.V. Radha, I. Regupathi, A. Arunagiri, T. Murugesan, Decolorization studies of synthetic dyes using Phanerochaete chrysosporium and their kinetics, Process Biochem., 40 (2005) 3337–3345.
[2] X.-Y. Yang, B. Al-Duri, Application of branched pore diffusion model in the adsorption of reactive dyes on activated carbon, Chem. Eng. J., 83 (2001) 15–23.
[3] D.F. Raymound EK, Encyclopedia of chemical technology, New York: Wily, (1984).
[4] M. Kucukosmanoglu, O. Gezici, A. Ayar, The adsorption behaviors of methylene blue and methyl orange in a diaminoethane sporopolleninmediated column system, Sep. Purif. Technol., 52 (2006) 280–287.
[5] K.M. Parida, N. Sahu, N.R. Biswal, B. Naik, A.C. Pradhan, Preparation, characterization, and photocatalytic activity of sulfate-modified titania for degradation of methyl orange under visible light, J. Colloid Interface Sci., 318 (2008) 231–237.
[6] J. Weber, C. Miller, Organic chemical movement over and through soil, Reactions and movement of org. chem. in soil., (1989) 305–334.
[7] M. A. Ghaedi, A. B. Ansari, M. H. C. Habibi, A. R. D. Asghari, Removal of malachite green from aqueous solution by zinc oxide nanoparticle loaded on activated carbon: Kinetics and isotherm study, J. Indus. Eng. Chem., 20 (2014) 17–28.
[8] M. A. Roosta, M.. A. Ghaedi, A. B. Daneshfar, R. B. Sahraei, A. C. Asghari, Optimization of the ultrasonic assisted removal of methylene blue by gold nanoparticles loaded on activated carbon using experimental design methodology, Ultrason. Sonochem., 21 (2014) 242–252.
[9] M. Ghaedi, A.M. Ghaedi, E. Negintaji, A. Ansari, F. Mohammadi, Artificial neural network-genetic algorithm based optimization for the adsorption of methylene blue and brilliant green from aqueous solution by graphite oxide nanoparticle, J. Indus. Eng. Chem., 20 (2014) 4332–4343.
[10] B.H. Hameed, I.A.W. Tan, A.L. Ahmad, Adsorption isotherm, kinetic modeling and mechanism of 2,4,6-trichlorophenol on coconut husk-based activated carbon, Chem. Eng. J., 144 (2008) 235–244.
[11] R. Jain, M. Shrivastava, Adsorptive studies of hazardous dye Tropaeoline 000 from an aqueous phase on to coconut-husk, J. Hazard. Mater., 158 (2008) 549–556.
[12] M. Nassar, K. Awida, E. Ebrahiem, Y. Magdy, M. Mehaedi, Fixed-bed adsorption for the removal of iron and manganese onto palm fruit bunch and maize cob, Adsorp. Sci. Technol., 21 (2003) 161–175.
[13] M. A. Roosta, M. A. Ghaedi, A. B. Daneshfar, R. B. Sahraei, Experimental design based response surface methodology optimization of ultrasonic assisted adsorption of safaranin O by tin sulfide nanoparticle loaded on activated carbon, Spectrochim. Acta - Part A: Molecu. Biomolecu. Spectros., 122 (2014) 223–231
[14] S. Karcher, A. Kornmüller, M. Jekel, Screening of commercial sorbents for the removal of reactive dyes, Dyes Pigm., 51 (2001) 111–125.
[15] S. Karcher, A. Kornmüller, M. Jekel, Anion exchange resins for removal of reactive dyes from textile wastewaters, Water Res., 36 (2002) 4717–4724.
[16] C.-H. Liu, J.-S. Wu, H.-C. Chiu, S.-Y. Suen, K.H. Chu, Removal of anionic reactive dyes from water using anion exchange membranes as adsorbers, Water Res., 41 (2007) 1491–1500.
[17] M.I. Khan, L. Wu, A.N. Mondal, Z. Yao, L. Ge, T.W. Xu, Adsorption of methyl orange from aqueous solution on anion exchange membranes: Adsorption kinetics and equilibrium, Mem. Water Treat., 7 (2016) 23–38.
[18] Y. Li, T. Xu, M. Gong, Fundamental studies of a new series of anion exchange membranes: Membranes prepared from bromomethylated poly(2,6-dimethyl–1,4-phenylene oxide) (BPPO) and pyridine, J. Mem. Sci., 279 (2006) 200–208.
[19] H.A. Chanzu, J.M. Onyari, P.M. Shiundu, Biosorption of malachite green from aqueous solutions onto polylactide/spent brewery grains films: kinetic and equilibrium studies, J. Polym. Environ., 20 (2012) 665–672.
[20] Z. Hu, H. Chen, F. Ji, S. Yuan, Removal of Congo Red from aqueous solution by cattail root, J. Hazard. Mater., 173 (2010) 292–297.
[21] S. Mohan, R. Gandhimathi, Removal of heavy metal ions from municipal solid waste leachate using coal fly ash as an adsorbent, J. Hazard. Mater., 169 (2009) 351–359.
[22] R. Gong, Y. Ding, M. Li, C. Yang, H. Liu, Y. Sun, Utilization of powdered peanut hull as biosorbent for removal of anionic dyes from aqueous solution, Dyes Pigm., 64 (2005) 187–192.
[23] Y.S. Ho, Adsorption of heavy metals from waste streams by peat, Ph.D. Thesis, University of Birmingham, Birmingham, (1995).
[24] N. Kannan, M.M. Sundaram, Kinetics and mechanism of removal of methylene blue by adsorption on various carbons—a comparative study, Dyes Pigm., 51 (2001) 25–40.
[25] Y.-S. Ho, Second-order kinetic model for the sorption of cadmium onto tree fern: A comparison of linear and non-linear methods, Water Res., 40 (2006) 119–125.
[26] M. Özacar, İ.A. Şengil, A kinetic study of metal complex dye sorption onto pine sawdust, Process Biochem., 40 (2005) 565–572.
[27] S. Chowdhury, R. Mishra, P. Saha, P. Kushwaha, Adsorption thermodynamics, kinetics and isosteric heat of adsorption of malachite green onto chemically modified rice husk, Desal., 265 (2011) 159–168.
[28] S. Kuo, E.G. Lotse, kinetics of phosphate adsorption and desorption by hematite and gibbsiti1, Soil Sci., 116 (1973) 400–406.
[29] C. Aharoni, M. Ungarish, Kinetics of activated chemisorption. Part 2.-Theoretical models, Journal of the Chemical Society, Faraday Trans.1: Phys. Chem. Condensed Phas., 73 (1977) 456–464.
[30] E. Tütem, R. Apak, Ç.F. Ünal, Adsorptive removal of chlorophenols from water by bituminous shale, Water Res., 32 (1998) 2315–2324.
[31] I.D. Mall, V.C. Srivastava, N.K. Agarwal, I.M. Mishra, Adsorptive removal of malachite green dye from aqueous solution by bagasse fly ash and activated carbon-kinetic study and equilibrium isotherm analyses, Colloids Surf. A: Physicochem. Eng. Aspec., 264 (2005) 17–28.
[32] B. Royer, N.F. Cardoso, E.C. Lima, J.C.P. Vaghetti, N.M. Simon, T. Calvete, R.C. Veses, Applications of Brazilian pine-fruit shell in natural and carbonized forms as adsorbents to removal of methylene blue from aqueous solutions—Kinetic and equilibrium study, J. Hazard. Mater., 164 (2009) 1213–1222.
[33] I. Langmuir, The constitution and fundamental properties of solids and liquids, J. Amer. Chem. Soc., 38 (1916) 2221–2295.
[34] T.W. Weber, R.K. Chakravorti, Pore and solid diffusion models for fixed-bed adsorbers, AIChE J., 20 (1974) 228–238.
[35] G. McKay, Adsorption of dyestuffs from aqueous solutions with activated carbon I: Equilibrium and batch contact-time studies, J. Chem. Technol. Biotechnol., 32 (1982) 759–772.
[36] L. Xiong, Y. Yang, J. Mai, W. Sun, C. Zhang, D. Wei, Q. Chen, J. Ni, Adsorption behavior of methylene blue onto titanate nanotubes, Chem. Eng. J., 156 (2010) 313–320.
[37] G. Annadurai, R. S. Juang, D. J. Lee, Use of cellulost-based wastes for adsorption of dyes from aqueous solutions, J. Hazard. Mater., B92 (2002) 263–274.

[38] A. Mittal, A. Malviya, D. Kaur, J. Mittal, L. Kurup, Studies on the adsorption kinetics and isotherms for the removal and recovery of Methyl Orange from wastewaters using waste materials, J. Hazard. Mater., 148 (2007) 229–240.
[39] Y. Yao, B. He, F. Xu, X. Chen, Equilibrium and kinetic studies of methyl orange adsorption on multiwalled carbon nanotubes. Chem. Eng. J., 170 (2011) 82–89
[40] Q. Ma, F. Shen, X. Lu, W. Bao, H. Ma, Studies on the adsorption behavior of methyl orange from dye wastewater onto activated clay. Desalin. Water Treat., 51 (2013) 3700–3709
[41] Y. Su, Y. Jiao, C. Dou, R. Han, Biosorption of methyl orange from aqueous solutions using cationic surfactant modified wheat straw in batch mode. Desalin. Water Treat., 52 (2014) 6145–6155
[42] R. Jiang, Y. Q. Fu, H. Y. Zhu, J. Yao, L. Xiao, Removal of methyl orange from aqueous solutions by magnetic maghemite/chitosan nanocomposite films: adsorption kinetics and equilibrium. J. Appl. Polym. Sci., 125 (2012) E540–E549.
[43] A. A. Jalil, S. Triwahyono, S. H. Adam, N. Diana Rahim, M. A. A. Aziz, N. H. H. Hairom, N. A. M. Razali, M. A. Z. Abidin, M. K. A. Mohamadiah, Adsorption of methyl orange from aqueous solution onto calcined Lapindo volcanic mud. J. Hazard. Mater., 181 (2010) 755–762
[44] Munagapati Venkata Subbaiah, Dong-Su Kim, Adsorption of methyl orange from aqueous solution by aminated pumpkin seed powder: Kinetics, isotherms, and thermodynamic studies, Toxicol. Environ. Safety, 128 (2016) 109–117
[45] H. Li, A. Nihong, L. Gang , L. Jialu, L. Na, J. Mingjun, Z. Wenxiang , Y. Xiaoling, Adsorption behaviors of methyl orange dye on nitrogen-doped mesoporous carbon materials, J. Colloid Interf. Sci., 466 (2016) 343–351.
[46] F. N. Allouche, N. Yassaa, H. Lounici, Sorption of methyl orange from aqueous solution on chitosan biomass, Procedia Earth Planetary Sci., 15 (2015) 596–601.
[47] E. H. Mekatel, S. Amokrane, A. Aid, D. Nibou, M. Trari, 2015. Adsorption of methyl orange on nanoparticles of a synthetic zeolite NaA/CuO, Comptes Rendus Chim., 18 (2015) 336–344
[48] M. J. Iqbal, M. N. Ashiq, adsorption of dyes from aqueous solutions on activated charcoal, J. Hazard. Mater. B139 (2007) 57-66.
[49] S. Chen, Q. Yue, B. Gao, Q. Li, X. Xu, Removal of Cr (VI) from aqueous solution using modified corn stalks: Characteristic, equilibrium, kinetic and thermodynamic study, Chem. Eng. J., 168 (2011) 909–917.
[50] R. Donat, A. Akdogan, E. Erdem, H. Cetisli, Thermodynamics of Pb 2+ and Ni 2+ adsorption onto natural bentonite from aqueous solutions, J. Colloid Interf. sci., 286 (2005) 43–52.
[51] B. Hu, H. Luo, H. Chen, T. Dong, Adsorption of chromate and para-nitrochlorobenzene on inorganic–organic montmorillonite, Appl. Clay Sci., 51 (2011) 198–201.